This project has received funding from the Euratom research and training programme 2014-2018 under grant agreement No 662287.

EJP-CONCERT

European Joint Programme for the Integration of Radiation Protection Research

H2020 – 662287

D 9.10 - Paper on external dosimetry using personal objects*

* Despite the title of the deliverable, this document is not a paper but a report

Lead Author: A. Mafodda (HMGU)

With contributions from: C. Woda (HMGU), J. Eakins (PHE)

Reviewer(s): C. Woda (HMGU)

and CONCERT coordination team

Work package / Task	**WP9**	**T9.1**	**ST 9.1.2**
Deliverable nature:	**Report**		
Dissemination level: (Confidentiality)	**Public**		
Contractual delivery date:	**M53 ->** postponed; New due date M54		
Actual delivery date:	**M54**		
Version:	**1.0**		
Total number of pages:	**19**		
Keywords:	**Nuclear emergency, retrospective dosimetry, personal items, external exposure, Monte Carlo simulations**		
Approved by the coordinator:	**M54**		
Submitted to EC by the coordinator:	**M54**		

.

Abstract

The present deliverable reports on research conducted on personal objects, such as electronic components of mobile phones (Surface Mounted Resistors), chip and memory cards, for their use as fortuitous dosimeters to measure the external exposure of an individual due to gamma radiation following a nuclear accident. For electronic components of mobile phones, the dosimetry methods for reconstructing individual doses have been optimized in the low dose-range (10 – 100 mGy), whereas for other materials the general use as a fortuitous dosimeter could be shown but application in the low dose range remains to be demonstrated. A methodology has been developed to derive organ absorbed doses from the measured doses in the materials using Monte Carlo simulations and is illustrated for selected radionuclides and exposure conditions relevant in a nuclear emergency. Major sources of uncertainty have been identified and quantified. The dosimetry tool could be applied in an efficient way, if targeted at critically exposed subgroups of the potentially affected population, which can be identified from environmental monitoring data, using individualized dose calculations.

Contents

1. Introduction 5
1.1 Individual dose assessment in case of a radiological or nuclear emergency 5
1.2 Luminescence dosimetry techniques using personal items 6
1.3 Dose conversion factors for emergency dosimetry 7
2. Materials and methods 7
2.1 RTL on single resistor 7
2.2 Chip cards and Memory Cards 8
2.3 MCNP simulations 8
3. Results 11
3.1 Resistors 11
3.2 Chip cards and memory cards 13
3.3 MCNP Simulations 15
4. References 18

1. Introduction

1.1 Individual dose assessment in case of a radiological or nuclear emergency

When a radiological or nuclear accident occurs, the scale may vary from small to large and in case of a large-scale emergency, a large number of individuals might be involved. Thus, in the early phase of the management of such an event, emergency dosimetry allows to evaluate the absorbed dose of exposed people and to enable rapid medical triage. Taking into account the expected limited availability of resources, it would be of major importance to define which patients will derive most benefit from prompt medical attention (*Ainsbury et al. 2011*). Radiation dose triage levels for symptoms and medical care (*Jaworska et al., 2014*) have been largely discussed in many scientific works. The most critical level, supported also by data from the Chernobyl victims, has been identified as 2 Gy of absorbed dose. In contrast to such high exposure conditions, doses to the population following a nuclear emergency are generally much lower. Nevertheless, the reconstruction of doses (and related uncertainties) to population is crucial to obtain a more consolidated picture of the radiological situation during the transition phase and to inform on necessary medical surveillance measures and medical screening needs. A sound dosimetry is also essential to better estimate the long-term health risk and to lay the basis for a possible epidemiological follow-up. As learned from the Fukushima Dai-ichi accident, when only order-of-magnitude dose bands from local contamination and model predictions were produced, individual doses, calculated either from monitoring data and taking into account individual behavior patterns or measured directly, could greatly reduce uncertainty and improve the accuracy of dosimetry. In this respect, individual retrospective dosimetry methods based both on biological and physical retrospective dosimetry techniques could potentially play a key role. The challenges in terms of sensitivity of the methods are however quite high, since in a nuclear emergency doses can be dominated by internal (inhalation and ingestion) doses and doses due to external exposure can be expected to be even lower. Nevertheless, it is exactly the external exposure that is so far often only estimated from environmental data and where individual dose measurement techniques are rarely applied or missing altogether.

Within WP2 of the CONFIDENCE project, a strategy was developed how environmental monitoring, individualized dose calculations based on these data and individual dose measurements can work together in the most effective way. From environmental monitoring, which is the first information at hand after passage of the radioactive plume, population groups potentially affected by high doses can be readily identified. For these (possibly still large) groups an individualized dose calculations can then be carried out (e.g. in emergency care centers), using dedicated software developed in the project and using information on the time spent in different contaminated areas (see Deliverable 9.7 for details). From these calculations, which can still be achieved in a comparatively short amount of time and with large capacity, a critically exposed subgroup can be identified. This subgroup is then subjected to individual dose measurements, which are more accurate than the dose calculations but more time consuming and usually available with less capacity. In this way, the limited resources of dose measurement techniques are used in the most efficient way.

This documents reports on the use of personal items as individual dosimeters for measuring the external exposure, with an emphasis on optimizing the performance in the low dose range and describes a methodology how these doses can be translated into organ absorbed doses for estimating health risks. These techniques are novel, still under development and as yet not part of any emergency dosimetry plans. With further consolidation and validation, they can become part of the toolkit used in the European network for biological and physical retrospective dosimetry (RENEB e.V.), which might be integrated into emergency response in the future (see also Deliverable D9.11).

1.2 Luminescence dosimetry techniques using personal items

As members of public, people are not usually equipped with proper devices for ionizing radiation monitoring. However, everyday objects can eventually perform as fortuitous dosimeters.

Dosimetric properties of some personal items represent both valuable and challenging resource of information during an emergency scenario. This explains why in the last decade, many investigations using different techniques were carried out on a wide range of different materials that are usually kept on or close to the human body: fabrics, cigarettes, money (paper and coin) and electronic devices (see *Bailiff et al.*, 2016 for a recent review and the upcoming joint ICRU-EURADOS report 94 (*ICRU*, 2019)).

Generally, a fortuitous dosimeter should meet several requirements to be useful in accident and retrospective dosimetry: it should show a unique and reproducible signal response to doses up to several Gy, no signal in the unexposed state, a lower detection limit of tens of mGy and allow dose assessment with reasonable accuracy up to several days after the exposure (*Woda et al.,2012*).

As measurement techniques, usually EPR (electron paramagnetic resonance), thermoluminescence (TL) and optically stimulated luminescence (OSL) is applied. Each of these are based on the principle that within certain materials, such as insulators and semiconductors, defects in the crystalline structure exists that form, metastable states in the forbidden region between valence and conduction bands. If the energetic gap between the ground state of the defect and one of those bands is sufficiently high, free charge carriers (electrons/holes), created from energy absorbed from exposure to ionizing radiation, might be trapped and accumulated during the whole irradiation time. The amount of trapped charges is directly proportional to the absorbed dose of the material. When stimulation is performed by heating (TL) or illuminating (OSL) the material, the trapped charges can be released (provided the energy is sufficient) and charge carriers of opposite sign recombine. Luminescent signals originate when the recombination process is radiative. In the past years, TL and OSL methods have been largely used for individual dosimetry on non-biological samples with a broad variety of results. Luminescence properties of dust from coins, keys, jewelry and tobacco from cigarettes indicated sensitivities in the range 100 mGy to 5 Gy (*Bortolin et al, 2011*). Lots of research effort was put into luminescence studies on personal electronic such as mobile phones, mainly due to their widespread use. The glassy amorphous material of phone display glasses and touchscreens have shown a TL signal strongly affected by a pre-existing native signal (*Discher, 2016; Discher and Woda, 2013*) and a sensitivity near to 1 Gy (compatible also with watch glasses). Even though their dose response curves were found to be linear over a wide dose range, for display glass the minimum detectable dose was assessed to 340 mGy and 100 mGy, for untreated and chemically etched samples, respectively. The detection limit are determined by the variability of the intrinsic background signal and as such a material property, which is not expected to change with future improvements in instrumentation. For touchscreen glass, improvement has been achieved using the Phototransfer-Thermoluminescence (PTTL) technique, but also here the detection limit varied strongly between samples, with values ranging from 0.1 to 5 Gy (McKeever *et al., 2017*). Also, chip cards modules integrated in bank cards, credit cards, health insurance cards and SIM cards have a side covered with epoxy, to which silicate material is added, which is suitable for OSL dosimetry. TL and infrared luminescence (IRSL) first studies observed a sensitivity change and a large “zero dose” affecting the signal. Blue-stimulated OSL allowed reaching higher sensitivity and a minimum detectable dose of ~20 mGy after 10 days, taking into account thermal and athermal fading. The electronic components placed on the circuit boards of phones and other portable devices, have been targeted for dosimetry applications too. SMR (surface mounted resistors), inductors and capacitors contain an alumina (Al_2O_3) substrate, that is sensitive to ionizing radiation. OSL and recently TL (in the blue wavelength range) studies have shown a detection

limit in the order of tens of mGy, linear dose response up to at least 10 Gy, and accurate correction factors for signal fading during the storage time (*Ademola and Woda, 2017*; *Lee et al.,2016; Fiedler and Woda, 2011, Ekendahl and Judas, 2012; Inrig et al., 2008; Mrozik et al., 2014*). Especially for resistors, different protocols to prepare and measure the samples are nowadays well known. Moreover tests on reconstructing pre-delivered unknown low doses (<1 Gy), medium doses (1–2 Gy) and high doses succeeded within 90% confidence (*Bassinet et al.,2014*). Limitations of applying this method in case of a nuclear emergency are the still too high detection limits (tens of mGy) and the fact that at least 10 components per phone have to be sampled, implying that the phone will be irreversibly destroyed by this procedure. This could lead to a low acceptability of the method.
In the next paragraphs, the study on new approaches on known materials (e.g. resistors) or the study on new materials will be presented to potentially overcome the mentioned issues.

1.3 Dose conversion factors for emergency dosimetry

In order for the absorbed doses measured by fortuitous dosimeters to be relevant, it is necessary to be able to relate them to the doses that are simultaneously received by the individuals that are "wearing" them. Within the context of CONFIDENCE, this suggests that the development of conversion factors between the two quantities would be strongly advantageous in attempts to reduce uncertainty in dose estimation, as would otherwise be propagated by naively assuming equivalence between measured physical doses and the concurrent biological doses to individuals. The above endeavour is particularly complicated by the expectation that the dose received by the retrospective dosimeter, such as a resistor within a mobile phone for example, will depend strongly on its location about the person (*Bossin, 2019; Discher, 2015; Eakins and Kouroukla, 2015; Kim, 2019; Kouroukla, 2015*). This dependence will be in addition to factors such as the precise energy and directional characteristics of the exposure, which will also determine the distribution of doses deposited in the various organs of the body. Any conversion factors between dosimeter and organ doses will therefore be multi-variable, which illustrates not only their complexity but also their critical importance for uncertainty reduction.

2. Materials and methods

2.1 RTL on single resistor

The red Thermoluminescence of the alumina substrates of resistors, extracted from the circuit board of different mobile phone models, was investigated as a possible new dose measurement method.

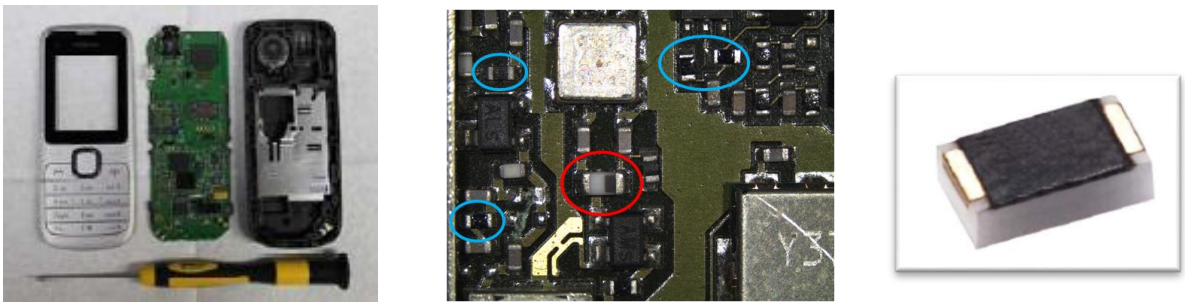

Figure 1- From left to right: example of a phone disassembled and detail of its circuit board where SMR (circled in blue) and inductors (circled in red) are found. On the left, a resistor zoomed.

In fact, preliminary spectral studies have shown that the TL signal due to the Cr^{3+} emission (695 nm) surpasses other emissions by two orders of magnitude (Lee et al., 2017). This dramatic increase in sensitivity was used here to develop a new protocol based on a single detector (single resistor of 1 mm x 0.5 mm) for the low dose region (10-100 mGy). In doing so, the issue of general acceptability of the method by the public is also addressed. A sampling procedure on a single component might enable its replacement after measurement, thus leaving the phone operational and intact. On the other hand, the full protocol (disassembling the phone - sampling - replacing the component - reassembling the phone) can be time-consuming and not suitable for triage dosimetry, i.e. processing a large amount of samples in the shortest amount of time possible. Thus, this approach seems primarily useful within the concept of targeting the critically exposed subgroup of the population, following a nuclear emergency, as outlined in section 1.1.

All the tests were carried out with Lexsyg Research luminescence reader $^{90}Sr/^{90}Y$ β source (dose rate ~20 mGy s^{-1}) and in dark light conditions to avoid any phototransfer process from deeper traps (*Ademola and Woda, 2017*). For trial irradiation, four intact mobile phones were irradiated free in air in air kerma reference conditions, with doses of 20 mGy, 40 mGy, 60 mGy and 100 mGy (air kerma value) using a ^{137}Cs source of the Secondary Standard Dosimetry Laboratory (SSDL) of the Helmholtz Zentrum München.

2.2 Chip cards and Memory Cards

Other personal items that are widespread, comparatively low-cost and easy replaceable are chip cards and memory cards (Figure 2). Chip cards have been investigated in several studies and the published results will be reported here. For memory cards, several tens of cards from different producers were collected for analysis. Measurements were carried out on intact cards and on the chemically extracted filler material, using a Risø TL/OSL-DA-15 and the same Lexsyg Research luminescence reader mentioned before, that is additionally equipped with an emission spectrometry unit.

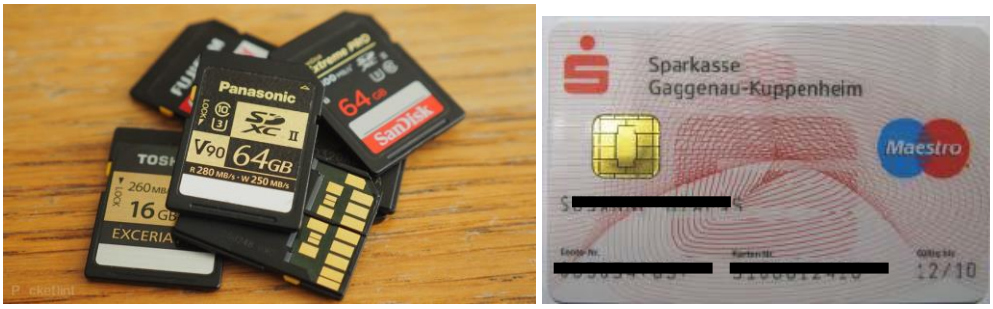

Figure 2 – Memory cards and bank card with chip

2.3 MCNP simulations

The general-purpose Monte Carlo radiation transport code MCNP6.2 (*Werner, 2017*) has been used to derive sets of appropriate conversion factor data. The overall approach has been to build a model of a realistic exposure scenario of relevance to accident dosimetry, and position an anthropomorphic phantom within that environment, about which representations of retrospective dosimeters are located; the dosimeter is identified here as the resistors within a mobile phone. Dose conversion factors can then be derived for each configuration by taking the ratios between the absorbed doses to the dosimeter and to the organs, where the values of these factors take as input the target organ of interest and the location of the phone.

As an illustration and proof-of-concept, a test exposure scenario was envisaged in which the individual is standing upon soil contaminated by a radionuclide. A schematic of the exposure configuration is shown in Figure 3.

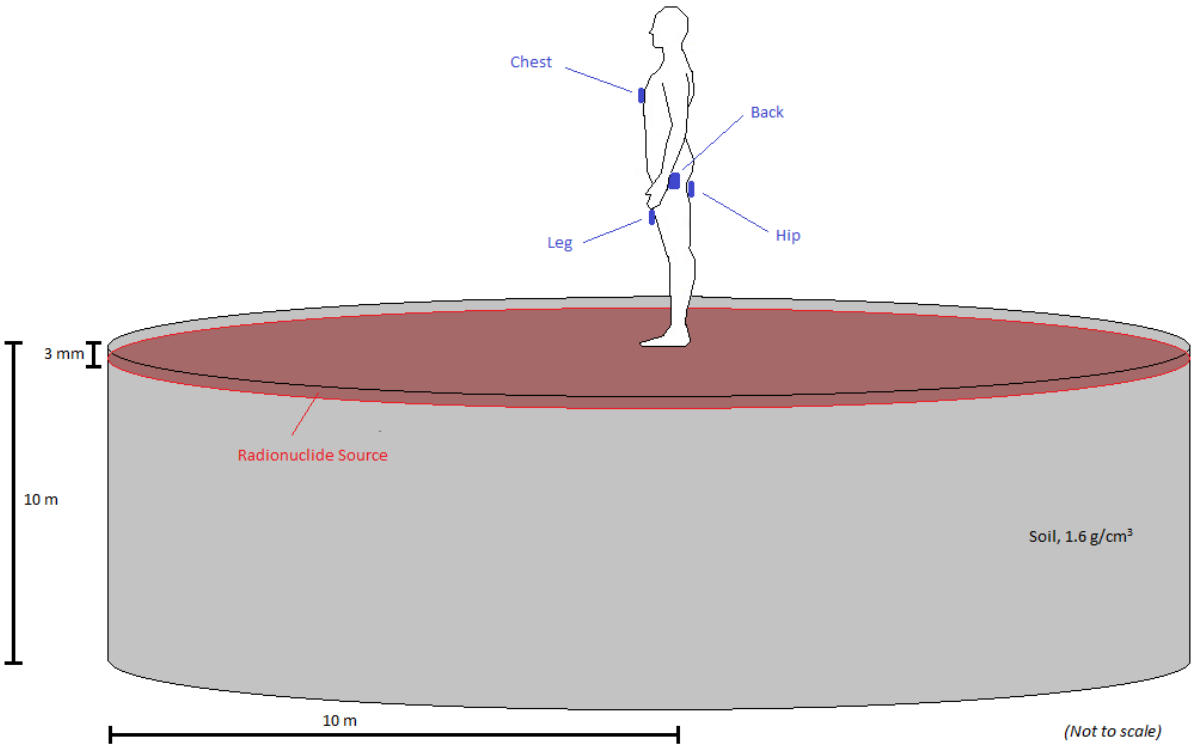

Figure 3 - Schematic of the modelled exposure scenario (not to scale)

The soil was assumed to be of density 1.6 g/cm^3 and chemical composition as defined in Table 1 (*Eckerman, 1993*), and was modelled as a homogenous cylinder of radius 10 m and depth 10 m.

Element	H	C	O	Al	Si	K	Ca	Fe
Mass Fraction	0.021	0.016	0.577	0.050	0.271	0.013	0.041	0.011

Table 1 - Composition of soil used in the modelling (Eckerman, 1993).

Such a geometry is essentially "infinitely deep" from the perspective of photon backscatter, whilst previous work (not shown here) has demonstrated that it is effectively infinite in radius from the perspective of an individual standing on top of its rotational axis, at least as a reasonable approximation: although wider cylinders could potentially have led to incrementally larger doses, the addition would reduce with the square of the radius, leading to vanishingly smaller contributions. From the perspective of the modelling, using radii larger than 10 m would therefore result in diminishing returns for proportionally longer calculation times, or equivalently, proportionally greater statistical uncertainties on the results from fixed-duration calculations with very little gain in systematic accuracy. Moreover, because the conversion factors are derived by taking dose ratios, any such small "missing" contributions are implicitly cancelled, and hence mitigated against.

The radionuclides used in the modelling were Cs-137 and I-131, because these are considered the most relevant gamma sources for nuclear emergency scenarios (*McKenna, 2017*). In the model, the radionuclide was assumed to be deposited uniformly in area within the soil at a depth of 3 mm (*Petoussi-Henss, 2012*). The ^{137}Cs was taken to emit monoenergetic photons at 662 keV, but for I 131 a realistic energy distribution was assumed with a main energy of ~360 keV (*Radiological Safety*

Guidance, 2018). Isotropic emission was assumed from the 3 mm deep source plane, with both direct and backscattered components therefore incident upon the individual, such that the energy distributions of the incoming photons differed from the 'raw' radionuclide fields.

MCNP normalizes all output data to per-source-particle, but because it is ratios of doses that are ultimately of interest, the results are appropriate for any arbitrary areal density of activity of these radionuclides.

For the doses to the individual, the ICRP Reference Male voxel phantom (*ICRP, 2008*) was introduced into the model, with its feet positioned just above the centre of the cylinder (Figure 1). The female phantom was not used, which had the obvious advantage of halving the number of calculations to be performed. One justification for this omission is that additional calculations using a female phantom would have yielded the illusion of an apparent improvement in accuracy that is not really defensible within the context of the overall large uncertainty budget inherent in the method. This budget includes factors such as the lack of any shielding due to the absence of clothes, and the clear departure from personalized dosimetry in the generation of the conversion factors due to the use of standardized reference phantoms that neglect features such as differences in height, weight or size from one individual to another. Regarding the last of these, being larger the male phantom is expected to demonstrate a greater range of dose inhomogeneity, and hence location-dependent conversion factors, than the female, and is hence better suited to demonstrate the significance and uncertainties of the overall approach, which further explains its preference over the female phantom in the modelling. Moreover, the dose enhancement factors provided in ICRP 116 (*ICRP, 2010*) and used to calculate red bone marrow (RBM) doses were derived using biological data for a male cadaver only.

To represent the retrospective dosimeters, a greatly simplified geometry was used in which they were modelled as thin cylinders of pure aluminium oxide of density 3.72 g/cm^3, with radius 0.564 cm and thickness 0.05 cm. This radius implies an effective area of ~1 cm^2, though this was chosen somewhat arbitrarily, whilst the thickness is commensurate with the height of a typical resistor within a mobile phone; the precise values of either of these are unlikely to impact the final results significantly, however. Aluminium oxide is employed as a substrate on integrated circuit boards, and is the active material used for both thermo-luminescence (TL) and optically-stimulated luminescence (OSL) dosimetry of resistors.

The decision not to surround the aluminium oxide cylinders by various plastic, glass or metal layers, or indeed model resistors accurately and incorporated within a fully realistic model of a complete mobile phone geometry, was based on several factors. The first of these is obviously simplicity. The second is that there are clearly many alternative designs of mobile phone currently on the market, all differing in shape, size, layout and composition, so choosing a universally consistent environment for their interiors would be problematic; likewise, resistors may be found (and hence extracted during measurements) in many different locations within a given phone, further confounding the choice of a single set of representative conditions for the modelling. And finally, and justifying the approximation, previous work in which a high-fidelity model of a real mobile phone was used (*Eakins and Kouroukla, 2015)* showed that the results were relatively insensitive to factors such as the orientation of the phone or the positions of resistors within it, indicating that differing attenuations of the photon fields by, for example, the phone's battery or display glass do not greatly impact the dosimetry. Simple field-attenuation analyses using mass-attenuation coefficients (*Hubbell, 1995*) for ~360 keV or 662 keV photons passing through ~1 cm of typical material predict and support this conclusion.

Four locations of the aluminium oxide cylinder about the body were considered (Figure 3). Taken as a set, it is suggested that the four configurations cover a number of the most likely places for mobile phones to be carried about the person when not in use. The locations were:

1. 'Chest', i.e. with the phone centred close to the location of the heart. This configuration is representative of a phone positioned in an inside jacket or breast pocket.
2. 'Leg', i.e. with the phone centred just in front of the left thigh. This configuration is representative of a phone positioned in a trouser front pocket.
3. 'Back', i.e. with the phone centred just behind the left buttock. This configuration is representative of a phone positioned in a trouser back pocket.
4. 'Hip', i.e. with the phone centred close to the left hip. This configuration is representative of a phone positioned either in the outside pocket of a jacket, or held in the left hand, or inside a handbag or shoulder bag with its strap over the left arm.

The approximate (x,z) positions, in centimetres, of the centres of the cylinders relative to the body's centre line (x=0) and the soles of the feet (z=0) were, respectively, (6, 131), (9, 76), (7, 88) and (19.5, 93); the y positions were such that the cylinders were nearly in contact with the skin at each location. In all cases, the rotational axes of the cylinders were such that they pointed perpendicularly away from the body. It is noted that only locations on the left side of the body are considered, for brevity; given the overall uncertainty budget, and the obvious observation that the above four options are just a very small fraction of the very large multitude of possible positions that phones could potentially be located, left-right symmetry of the body may reasonably be assumed when subsequently applying the conversion coefficients. The Monte Carlo calculations were performed by making the kerma approximation and using photon-only transport ('mode p'), with secondary charged particle equilibrium assumed at all points-of-test and justified from a consideration of maximum expected ranges of electrons within the geometry (*ICRU, 1984*). This decision was made due to the significant advantages of mode p calculations over coupled electron-photon transport in terms of simulation efficiency, especially given the large spatial extent of the voxel geometry, with no significant impact on the accuracy of the results anticipated. Doses to the aluminium oxide cylinders, and to most organs within the body, were determined using MCNP f6:p photon kerma tallies. The exception was the dose to the red bone marrow (RBM), for which fluence tallies were used in conjunction with energy-dependent weighting factors that take account of dose enhancement within the bone according to the method recommended by ICRP 116 (*ICRP, 2010*).

3. Results

3.1 Resistors

In order to deal with systematic changes in sensitivity observed in own investigations done in the same detection window, the sample preparation was optimized. Propanol was used to remove any residuals of solder mask on the resistors and the maximum readout temperature was lowered from 400°C to 350°C.

When using a single small sized detector, one possible source of uncertainty is the detection limit. For testing the protocol, dose recovery tests were performed on single resistors extracted from a Samsung model of 2011. For the dose region from 1.2 Gy down to 80 mGy, nominal and given doses agree within 10%, however for the lowest two doses tested (40 and 60 mGy), the deviation increases up to ~50% or, in absolute terms, amounts to ~25 mGy (Table 2). Individual dose errors were calculated from the scatter of the data points around the calibration curve and by propagating the uncertainties of the

fitting parameters. An example of a calibration curve is given in Fig. 2. The comparison of the calculated errors with the observed deviation in Table 2 implies that the true uncertainties are underestimated.

Given Dose [mGy]	Recovered dose [mGy]	Error
1200	1170,37	±3,30
500	533,59	±3,69
200	216,50	±2,78
120	123,87	±1,96
80	85,65	±2,00
60	86,76	±2,14
40	53,09	±1,74

Table 2 – Results on reconstructing different doses with RTL measurement on single resistor

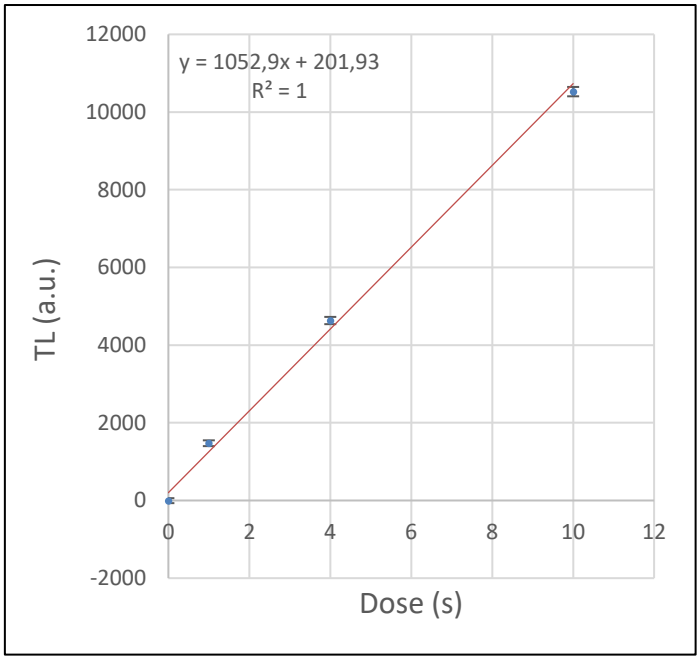

Figure 4 – Example of calibration curve for reconstructing 40 mGy dose. The dose on the x-axis is given in irradiation time of the built-in beta calibration source of the luminescence reader. 2 s approximately correspond to 40 mGy.

When using the built-in calibration source of the reader, an additional dose introduced from the time-dependent offset intrinsic to the machine has to be considered for the shortest irradiation times. In fact, the mechanical actions of opening/closing the beta source requires more time than what is recorded as irradiation time. To estimate the impact of this potential source of uncertainty, several experiments to determine the offset of the instrument were conducted, also on TLD detectors, yielding a value of (5.4 ± 2.3) mGy.

Furthermore, alumina porcelain substrates of SMRs within a phone are affected by a strong zero-dose signal in the higher temperature range (320°C) that might interfere with the dosimetric signal. A possible explanation for the origin of the zero-dose signal lies in the black overcoat of the thin film resistors, which is made up to 75% of an epoxy resin that is cured by UV light during the production process (*Ademola and Woda, 2017*).

Working with one single detector allow assessing if the distribution of such zero-dose is inhomogeneous among the components of the circuit board and if the value depends on where the sample is taken from. To investigate this, five different phone models were sampled from different position on the circuit board (top – middle - bottom) with a total amount of 35 resistors. Two of them

were considered as outliers (70 mGy) whereas most of them showed a zero-dose value relatively close to the detection limit. The same result was observed when comparing different models.
A fading rate study conducted on resistors sampled within one phone and between different phone models showed a variability of fading rate of around 20%. In Figure 5, the fading curves for two resistors extracted from the same phone, Samsung Fame, are shown.

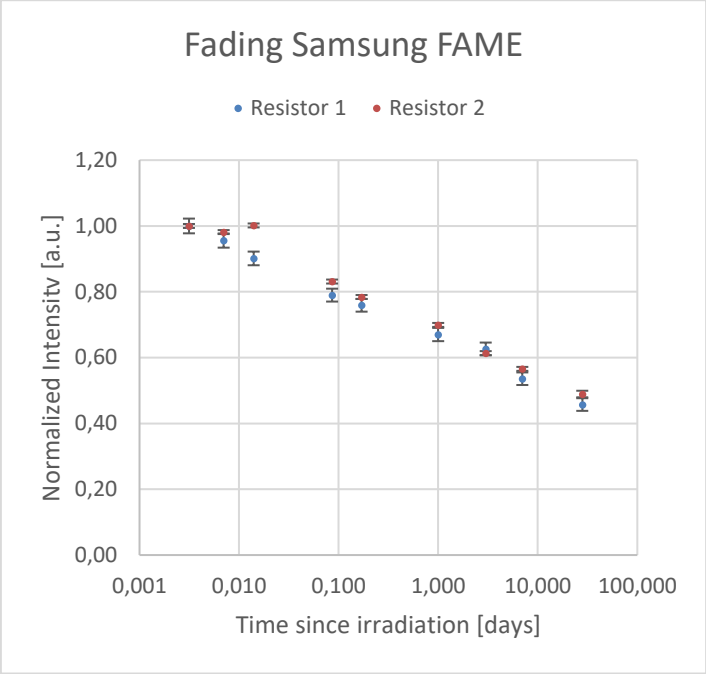

Figure 5 – Example of fading curve for two resistors from Samsung FAME

In addition, for trial irradiation, intact mobile phones were irradiated free in air in air kerma reference conditions with doses of 240 mGy ,100 mGy, 60 mGy, 40 mGy and 20 mGy (air kerma value) using a Cs-137 source of the Secondary Standard Dosimetry Laboratory (SSDL) of the Helmholtz Zentrum München. Measurements of the samples were performed some days after irradiation (the latest one one month after irradiation), since in a real case scenario a time delay between accident and sample collection might be of the same order (days). After fading correction, dose reconstruction was successful for all samples.

3.2 Chip cards and memory cards

Chip cards

The dose-response curves for all types of chip encapsulations investigated in the literature was linear up to at least 10 Gy. For UV-cured chip encapsulations, measurements were done at room temperature, without a preheat, to minimize the influence of confounding signals. For chemically prepared molded encapsulations, a preheat of 150 °C for 20 s and OSL measurement at 140 °C was proposed, to compensate for signal loss due to elevated temperatures during preparation. Different OSL readout times and integration intervals for both signal and the background have been reported in the literature. Generally, readout times (i.e. stimulation times) were chosen according to the shape of the OSL signal and were sufficiently long to avoid possible signal recuperation and reduced reproducibility effects (Cauwels et al., 2010; Woda and Spöttl, 2009). In some UV-cured chip card modules, moderate sensitivity changes up to 20% have been observed, while in other samples no sensitivity changes were seen.

The minimum detectable dose immediately after irradiation was assessed as 2-7 mGy for UV-cured transparent encapsulations, 40-60 mGy for intact contact-based molded encapsulation and 3 mGy for chemically prepared molded encapsulation. These values increase to 20-40 mGy, 130 mGy and 5 mGy, respectively for dose measurements performed 10 days after irradiation, due to signal fading.
Dose recovery tests were carried out for UV-cured encapsulation under idealized conditions, using the same in-built beta source of the luminescence reader for both the simulated accident and the calibration dose(s). OSL measurements were performed immediately and up to six days after irradiation. In each case, the obtained (fading corrected) doses were reported to be within 10-15% of the given doses (Cauwels et al., 2010; Woda and Spöttl, 2009). For molded encapsulations, laboratory irradiation using a ^{137}Cs source gave reasonable agreement for both intact and prepared modules and for measurements made promptly after irradiation. However, a systematic underestimation by 30% was observed for measurements after several days using prepared modules (Woda et al., 2012).

Memory cards

For memory cards, repeated cycles of irradiation and OSL-readout resulted in an increase of radiation sensitivity. The change in sensitivity was only dependent on the accumulated dose, not on the number of cycles. For dose measurement, a single aliquot regenerative dose (SAR) protocol was used. Due to the increase in sensitivity, the dose response was at first supralinear. In a first step, it was tried to correct for this by normalizing the measured OSL signal to the OSL response to a fixed test dose, a procedure that is routinely and very successfully applied in quartz dating (Murray and Wintle, 2003). Here, however, this lead to an over-correction of the sensitivity change and apparent saturation of the signal. By additionally introducing a post-heating (background reduction) and bleaching step (thermal transfer reduction), a linear dose response was obtained (Figure 6).

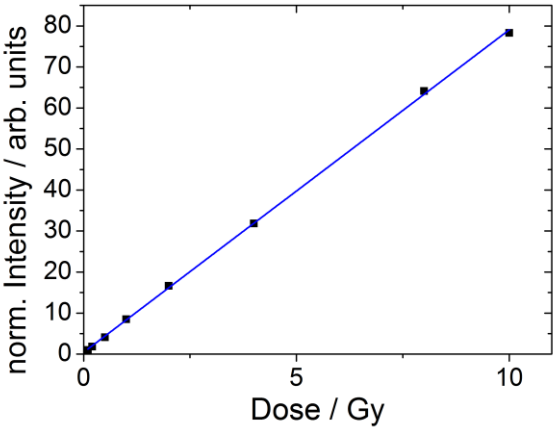

Figure 6 – Dose response curve of a memory curve measured using the developed protocol

In a radiological scenario, time elapses between irradiation and readout. The OSL signal of memory cards was seen not to be stable at room temperature but faded with time, showing the characteristic of anomalous fading. A multiple aliquot method was used and the following type of function fitted to the data for fading correction:

$$f(t) = a - b \cdot \ln(t).$$

The detection limit immediately after irradiation was estimated at 20-40 mGy. The sensitivity to radiation can be significantly increased and consequently the detection limit lowered, if the dosimetry is carried out not on the intact cards but on the chemically extracted filler materials. The principal

possibility of such an approach could be demonstrated but a full testing of the extracted filler as a dosimeter needs to be accomplished in future studies.
Trial irradiations were conducted both on punched out memory cards with the inbuilt beta-source of the Risø reader and on cards placed inside a phone with a ^{137}Cs source of the Secondary Standard Dosimetry Laboratory of the research center. Given doses were 2 and 5 Gy and doses were reconstructed after two to five days storage using the suggested readout protocol and fading correction. 12 out of 14 doses were reconstructed successfully.

3.3 MCNP Simulations

The conversion factor, $C_{P\rightarrow O}^{L}$, from phone dose, D_P^L, to organ dose, D_O, is obtained from the simple ratio:

$$C_{P\rightarrow O}^{L} = D_O / D_P^L$$

where the superscript 'L' reminds that the value is dependent on the location of the phone. Taken in the above form, the measured dose to a phone may be multiplied by the conversion factors to provide the concurrent doses to the organs of interest, using knowledge of the phone's location as an input variable. The conversion factors formally have units of (Gy/Gy), but are effectively dimensionless.

Values for $C_{P\rightarrow O}^{L}$ are provided for ^{137}Cs in Table 2 and for ^{131}I in Table 3.

	Conversion Factor, $C_{P\rightarrow O}^{L}$ (Gy/Gy)			
Location, *L*	*Colon*	*Thyroid*	*Breast*	*RBM*
Chest	0.99 (0.03)	0.84 (0.03)	1.03 (0.03)	0.90 (0.02)
Leg	0.74 (0.02)	0.63 (0.02)	0.77 (0.02)	0.68 (0.02)
Back	0.81 (0.02)	0.68 (0.02)	0.84 (0.02)	0.74 (0.02)
Hip	0.82 (0.02)	0.70 (0.02)	0.86 (0.03)	0.75 (0.02)

Table 2 - Conversion factors, $C_{P\rightarrow O}^{L}$, for Cs-137 ground contamination for four organs: colon, thyroid, breast and RBM. Bracketed values denote 1 standard uncertainty.

	Conversion Factor, $C_{P\rightarrow O}^{L}$ (Gy/Gy)			
Location, *L*	*Colon*	*Thyroid*	*Breast*	*RBM*
Chest	0.93 (0.03)	0.78 (0.02)	0.98 (0.03)	0.84 (0.02)
Leg	0.71 (0.02)	0.60 (0.02)	0.75 (0.02)	0.64 (0.02)
Back	0.76 (0.02)	0.64 (0.02)	0.80 (0.02)	0.69 (0.02)
Hip	0.78 (0.02)	0.66 (0.02)	0.82 (0.02)	0.70 (0.02)

Table 3 - Conversion factors, $C_{P\rightarrow O}^{L}$, for I-131 ground contamination for four organs: colon, thyroid, breast and RBM. Bracketed values denote 1 standard uncertainty.

Absorbed dose data for all organs were generated, but for brevity only conversion factors for the RBM, colon, breast and thyroid are shown due to their critical importance to radiation risk assessments following nuclear accident scenarios. Note that these four organs are positioned fairly symmetrically within the body relative to its left-right orientation, which further supports the assertion that placing all four phone locations just on the left of the body will still yield conversion factors that are likely to be appropriate for both sides. The uncertainties on the data in Tables 2 and 3 represent one standard deviation, and indicate combined statistical uncertainties just from the Monte Carlo modelling itself, which is an inherently stochastic process. Systematic uncertainties are not included.
Analyses of Tables 2 and 3 exhibit anticipated trends, readily explainable from a consideration of the exposure conditions and the distributed positionings of the various phones and organs around the

geometry. Within each table, for instance, conversion factors for the Chest phone are closer to unity than for the other locations, as expected due to its slightly closer proximity to the organs within the body. Conversely the value of $C_{P\rightarrow O}^{L}$ tends to reduce as the phone location becomes closer to the ground, and hence closer to the radionuclide source, with the phone on the leg exhibiting the largest relative dose and thereby giving rise to the smallest conversion factors. Moreover, all the conversion factors for I 131 are lower than their counterparts for Cs 137, as expected because the mean energy of the former distribution is significantly lower than the 662 keV photons of the latter, so the field is attenuated more by the body. The I 131 exposure is therefore less penetrating: like-for-like organ doses are hence much lower for I 131 than for Cs 137, whilst the phones, being located externally, exhibit less drastic differences in their doses. For a similar reason, being located at a shallower depth the breast receives higher doses than the other organs within each of the two datasets, so the factors converting to it are typically a little higher. It should be noted that although none of these patterns are critical in themselves for emergency dosimetry, their agreement with anticipated trends demonstrates confidence in the approach, and correct observation of them is hence an important part of the quality assurance process for the modelling.

The statistical uncertainties given in Tables 2 and 3 are sufficiently low for the present purposes (<few %, at 1 standard deviation), but could be made arbitrarily lower by running the calculations for longer, albeit with diminishing returns: Monte Carlo precision typically scales with the square-root of the computational time. The current exclusion of systematic uncertainties in the work is harder to mitigate. However, this partially reflects the situation in reality: in a genuine radiological emergency, many sources of systematic uncertainty, such as the precise location of the phone about the body, will likely be unknown so a broad approach to taking them into account would inevitably be necessary. Indeed, whilst the systematic uncertainties in the modelled results are themselves unquantified, it should be recalled that these calculations have been performed with the sole intention of evaluating and correcting for the effect of phone location in order to reduce uncertainties. In that regard, by considering all the data in Tables 2 and 3, the overall systematic uncertainty resulting from total ignorance of a phone's location across the whole body is seen to up to a few 10s of percent, so small translocations around the four positions considered here are likely to have far smaller impacts. Interpreting the data in Tables 2 and 3 as being sufficiently representative of general areas of the body, rather than just four precise positions, might therefore only be expected to lead to small misestimates of organ doses. Other systematic uncertainties for the phones, such as those arising from the neglection of their physical construction, are expected to be small as discussed previously (*Eakins, 2015*). Variations in the density or composition of the soil away from the parameters adopted in the present work (Table 1), or changes to the depth at which the radionuclide is deposited from the nominal 3 mm considered here, have the potential to affect individual phone and organ doses significantly. However, the impact of these on the doses might be expected to be fairly global, so would likely cancel to some extent when ratios are taken, and hence have much less influence on the conversion factors themselves. Alternative configurations for evaluating doses to individuals, such as via use of the smaller female phantom or by the inclusion of heavy clothes that could partially shield the organs to a greater extent than the phones, could also impact upon the conversion factors. Nevertheless, the current set-up is considered to represent a scenario that is maximally conservative. Consequently, using the data in Tables 2 and 3 to perform phone dose conversions for females or for clothed individuals would likely lead to results that over-estimate, rather than under-estimate, the true organ doses. Whilst not ideal, this is of course preferable to the converse. The current work serves as a successful demonstration and proof-of-concept for the overall methodology for generating phone to

organ dose conversion factors for use with emergency retrospective dosimetry. Attention has focussed here on the examples of Cs 137 and I 131 exposures, but the approach is readily expandable to other radionuclides of relevance to ground contamination scenarios following accidents. With the overall approach now established, such an extension will form the basis of future work. The data in Tables 2 and 3 may be employed to convert the absorbed doses measured using the resistors within phones to the absorbed doses to the four most important organs, thereby providing more accurate estimates of radiation risk for individuals. Four generic phone locations have been considered, corresponding to those areas where phones are most likely to be carried on the person when not in use, though this essentially doubles because left-right symmetry of the phones' locations about the body is assumed. For phones not in any one of these four general areas, which could be the case in some real emergency scenarios, the generic conversion factors of Tables 2 and 3 may still be used, with an approach naturally envisaged in which the choice of dataset is made based on whichever relates to the position closest to the actual phone location. Interpolating datasets, averaging, or erring on conservatism, are alternative approaches that could be potentially adopted in such circumstances, as appropriate. It is clear from Tables 2 and 3 that ignorance of the location of the phone during a ground contamination exposure to ^{137}Cs or ^{131}I, or equivalently neglecting to correctly apply a conversion factor from phone to organs doses, would lead to uncertainties of up to several tens of percent being introduced into the retrospective dosimetry method. Within the context of CONFIDENCE, this is an important observation, and re-emphasizes the obvious point that doses to phones are not the same thing as doses to individuals and should not be interpreted synonymously.

4. Summary and conclusions

The scientific work reported in this deliverable illustrates how individual retrospective dosimetry, combined with environmental monitoring data and individualized dose calculations, might play a crucial role in the transition phase of a nuclear emergency. In particular, personal items were targeted for investigations on their usability as fortuitous personal dosimeters, using new techniques (e.g. red Thermoluminescence on mobile phones resistors) or exploring new materials (e.g. memory cards). Dose measurement protocols were optimized in the low dose range to evaluate their effectiveness in case of a nuclear emergency scenario, where most of the population would be affected by an unplanned external exposure of comparatively low doses. Moreover, since such dose assessments involved objects of high personal value (such as smartphones), the concept of possible acceptability of the methods by the population was addressed. The red Thermoluminescence of the alumina substrates of resistors, extracted from the circuit board of different mobile phone models, represents a promising technique in this respect, as it potentially allows a non-destructive measurement approach. Major sources of uncertainties in the dose assessment using RTL of surface mounted resistors are the variation of the intrinsic background signals in the material, the variability in the time-offset of the calibration source and the variability in fading rates. Next to the experimental work, MCNP simulations were run in order to develop a methodology to translate the measured doses in the material into organ absorbed doses. From this investigation, an overall systematic uncertainty of the 20% arised when the location of the phone on the body was unknown. External dosimetry using resistors from mobile phones in a potentially non-destructive approach could thus be possible with an estimated overall uncertainty of 30-50%. Reconstructing doses with less valuable personal items, such as memory cards, was successful for doses of and above 2 Gy. In this case, protocols for the low dose range need to be further investigated by using the filler material to increase sensitivity.

5. References

- Cauwels, V., Beerten, K., Vanhavere, F., and Lievens, L. (2010). “Accident dosimetry using chip cards” In "Third European IRPA Congress", pp. 866-874, Helsinki, Finnland.
- Woda, C., and Spöttl, T. (2009). "On the use of OSL of wire-bond chip card modules for retrospective and accident dosimetry”, Radiat. Meas 44, 548-553
- Fiedler, I., and Woda, C. (2011). "Thermoluminescence of chip inductors from mobile phones for retrospective and accident dosimetry", Radiat. Meas. 46, 1862-1865.
- Ekendahl, D., and Judas, L. (2012). "Retrospective dosimetry with alumina substrate from electronic components", Radiat. Prot. Dosim. 150, 134-141.
- Inrig, E.L., Godfrey-Smith, D.I., and Khanna, S. (2008). "Optically stimulated luminescence of electronic components for forensic, retrospective, and accident dosimetry", Radiat. Meas. 43, 726-730.
- Mrozik, A., Marczewska, B., Bilski, P., and Gieszczyk, W. (2014). "Investigation of OSL signal of resistors from mobile phones for accidental dosimetry", Radiat. Meas. 71, 466-470.
- Ademola, J., Woda, C. (2017). “Thermoluminescence of electronic components from mobile phones for determination of accident doses”, Radiat. Meas. Volume 104 – pp 13-21
- Ainsbury et al. (2011). “Review of retrospective dosimetry techniques for external ionizing radiation exposures”, Radiat. Prot. Dosim. 147, 573-592
- Bailiff, I.K., Sholom, S., and McKeever, S.W.S. (2016). “Retrospective and emergency dosimetry in response to radiological incidents and nuclear mass-casualty events: A review”, Radiat. Meas. 94, 83-139.
- Bassinet et al. (2014). “Radiation accident dosimetry: TL properties of mobile phone screen glass”, Radiat. Meas. 71, 461-465.
- Bortolin et al. (2011). “Silicates collected from personal objects as a potential fortuitous dosimeter in radiological emergency”, Radiat. Meas. 46, 967-970.
- Bossin (2019). “New fortuitous materials for luminescence dosimetry following radiological emergencies”, Doctoral thesis, Durham University.
- Discher (2015). „Lumineszenzuntersuchungen an körpernah getragenen Gegenständen für die Notfalldosimetrie“ (in German), München, Technische Universität, Fakultät für Physik, Dissertation, 128 S.
- Discher, M., Bortolin, E., Woda, C. (2016). ”Investigations of touchscreen glasses from mobile phones for retrospective and accident dosimetry”, Radiat. Meas. 89, 44-51.
- Eakins and Kouroukla (2015). “Luminescence-based retrospective dosimetry using Al2O3 from mobile phones: a simulation approach to determine the effects of position” J. Radiol. Prot. 35, pp 343–381.
- Hubbell (1995). “Tables of X-Ray mass attenuation coefficients and mass energy-absorption coefficients from 1 keV to 20 MeV for elements Z = 1 to 92 and 48 additional substances of dosimetric Interest” NIST Report: NISTIR 5632.
- International Commission on Radiological Protection (ICRP), (2008). Adult Reference Computational Phantoms. ICRP Publication 110.
- International Commission on Radiological Protection (ICRP), (2010). Conversion Coefficients for Radiological Protection Quantities for External Radiation Exposures. ICRP Publication 116

- International Commission on Radiation Units and Measurements (ICRU), (2019). Methods for Initial-Phase Assessment of Individual Doses following Acute Exposure to Ionizing. ICRU Report 94 (International Commission on Radiation Units and Measurements, Bethesda, MD).
- International Commission on Radiation Units and Measurements (ICRU) (1984). Stopping powers for electrons and positrons. ICRU Report 37 (International Commission on Radiation Units and Measurements, Bethesda, MD).
- Jaworska et al. (2014) "Types of radiation mass casualties and their management", Ann Ist Super Sanità 45, 246-250.
- Kim (2019) "A study on dose conversion from a material to human body using mesh phantom for retrospective dosimetry" Radiat. Meas. Volume 126, July 2019, 106126
- Kouroukla (2015). "Luminescence dosimetry with ceramic materials for application to radiological emergencies and other incidents", Doctoral thesis, Durham University.
- Lee et al. (2016). "Dose re-estimation using thermoluminescence of chip inductors and resistors following the dose estimation by using optically stimulated luminescence readout for retrospective accident dosimetry", Radiat. Meas. 90, 257-261.
- McKenna (2017). "Operational Intervention Levels for Reactor Emergencies", IAEA Report EPR-NPP-OILs.
- Petoussi-Henss (2012). "Organ doses from environmental exposures calculated using voxel phantoms of adults and children", Phys. Med. Biol. 57, 5679–5713
- Radiological Safety Guidance, 2018 Iodine-131. Department of Environment, Health and Safety, University of Michigan.
- Werner (2017). "MCNP Users' Manual, version 6.2" Los Alamos National Laboratory (LANL) report: LA-UR-17-29981.
- Woda et al. (2012). "On the use of OSL of chip card modules with molding for retrospective and accident dosimetry", Radiat. Meas. 47, 1068-1073.